22nd AIAA International Communications Satellite Systems Conference & Exhibit 2004
9 - 12 May 2004, Monterey, California

AIAA 2004-3145

Jitter Control of Space and Airborne Laser Beams

R. Joseph Watkins * and Brij N. Agrawal.†
Department of Mechanical and Astronautical Engineering, Naval Postgraduate School, Monterey, CA, USA 93943

Young. S. Shin ‡
Department of Mechanical and Astronautical Engineering, Naval Postgraduate School, Monterey, CA, USA 93943

and

Hong-Jen Chen §
Department of Mechanical and Astronautical Engineering, Naval Postgraduate School, Monterey, CA, USA 93943

Acquisition, Tracking and Pointing (ATP) of space and airborne laser beams is fast becoming an important research topic as requirements for the pointing and control of the optical beam is increasing. Arc-second accuracy, nano-radian jitter and large flexible structures combine to require stringent pointing requirements testing the limits of control systems. Solar arrays, reaction wheels, control-moment-gyros for spacecraft and airframe, engine, and payload configuration for aircraft result in narrowband as well as random structural interactions that further complicate the control method. Additionally, the effect of the atmosphere on the laser adds a broadband disturbance, resulting in a laser beam that has been corrupted by "colored noise". This paper will focus on the control techniques that may be used to remove the disturbances. A Laser Beam Jitter Control test bed (LJC) has been developed at the Naval Post Graduate School and is used to investigate different control algorithms for Fast Steering Mirrors (FSM). The test bed consists of two FSMs, three position sensing detectors (PSD), one diode laser, and several beam splitters and mirrors, all sitting on a vibrationally isolated Newport optical bench. The control mirror, along with beam splitters and folding mirrors, is mounted on a platform isolated from the optical bench. The platform is shaken by a CSA SAS-5 (5 lb.) inertial actuator. Colored noise is injected with one FSM and the other FSM is used to control it. The disturbance spectrum contains not only narrow band noise from the shaken platform simulating rotating devices onboard such as reaction wheels but also broadband noise from a disturbance FSM, separate from the platform. Several adaptive feedforward and feedback control algorithms are tested with this disturbance on the LJC and are compared.

Nomenclature

DFSM	=	Disturbance Fast Steering Mirror
D_m	=	distance from control mirror to target, m
FSM	=	Fast Steering Mirror
G_m	=	mirror gain, rad/V
G_p	=	detector gain, m/V
H_d	=	detector transfer function
H_m	=	mirror transfer function
LJC	=	Laser Jitter Control
μ	=	adaption step size

* PhD Student, Department of Mechanical and Astronautical Engineering, e-mail: rjwatkin@nps.edu.
† Distinguished Professor and Director, Spacecraft Research and Design Center, Department of Mechanical and Astronautical Engineering, e-mail: agrawal@nps.edu. Associate Fellow, AIAA.
‡ Professor, Department of Mechanical and Astronautical Engineering, e-mail: yshin@nps.edu.
§ NRC Research Assistant, Department of Mechanical and Astronautical Engineering, e-mail: hchen@nps.edu. Member, AIAA.

M = number of tap gains
n = sample number
P = cross-correlation vector, desired to input
R = input auto-correlation matrix
R = weighting matrix for cost function
RFSM = Receive Fast Steering Mirror
s = Laplace variable
θ = rotation about control mirror axis, rad
θ_d = rotation about laser axis at source (disturbance)
T = time constant for circuitry
u = vector of delayed inputs
V_m = voltage command to mirror, V
V_p = voltage detected at PSM
W = vector of tap gains
w_n = natural frequency, rad/s
ζ = damping ratio

I. Introduction

THE ability to accurately point a laser beam is becoming increasingly important. The use of satellites to relay laser communications through space and from/to earth could increase available bandwidth and thus data transfer rate by several orders of magnitude. The use of lasers as defensive weapons, especially against missile systems, will require extremely accurate pointing capabilities. Jitter, the undesired fluctuations in the pointing of a laser beam due to environment or structural interactions, reduces the intensity of the beam at the target, whether the beam is used as a communications system or a weapon. For example, a 100 mm diameter beam with 1 mrad of jitter will result in roughly a 100 fold decrease in the intensity of the beam at 500 km, due to the jitter alone. This paper summarizes the development of the Optical Relay Mirror Lab – Laser Jitter Control (LJC) Testbed, which is located in the Spacecraft Research and Design Laboratory at Naval Postgraduate School. During the first phase of the research, classical control techniques are implemented to learn how the system behaves from a classical viewpoint. Next, proven adaptive means are implemented and compared to the ideal Wiener Filter, as well as to each other and the classical control model on colored noise provided by the disturbance FSM. In the third phase, the platform containing the control system is shaken to evaluate the effectiveness of various systems to onboard disturbances.

II. Experimental Platform and Mathematical Model

A. Experimental platform – Laser Jitter Control (LJC) Testbed

The LJC Testbed is constructed around two FSMs and three PSMs. A block diagram showing the arrangement is provided in Figure 1. The laser source is a 2.5 mW, 670nm diode laser. Disturbance injection is accomplished by a FSM, purchased from Baker Adaptive Optics[1], denoted as the DFSM. The Receive FSM (RFSM) was purchased from Newport Corporation[2]. The function of these two mirrors may be easily exchanged. The experimentally determined control bandwidth of the mirrors was found using spectrum analysis to be approximately 800 Hz for the Newport mirror in both axes and about 4 kHz for the Baker mirror in both axes. The Newport mirror provides a voltage output proportional to the position of the mirror, however, the Baker mirror does not. The computer control system is based on MATLAB release 13 and the xPC Targetbox, all from the Mathworks[1]. The xPC Targetbox has the ability to accept 16 differential inputs and provide 4 analog outputs. The main computer for control implementation and experiment supervision is a 2.4 GHz Dell with 1 Gbyte of RAM.

The sensors, known as Position Sensing Modules or PSMs, were purchased from OnTrak Photonics Inc.[2] and have a detection area of 10mm x 10mm. Each Position Sensing Module (PSM) requires an amplifier, the OT-301. The combination of amplifier and detector is called a Position Sensing Detector (PSD).Various beam splitters and folding mirrors are used to direct the beam as desired. The detectors have a minimum sensitivity of 50-100 mW, which drives the selection of the beam splitters and the determination of laser power. The optimum beam size for accurate detection on the PSM is between 1 and 3 mm, and the maximum allowed intensity should be less than 300 W/cm^2. The output range of the PSM/OT-301 detector is plus or minus 10 V and the OT-301 amplifier has a noise level of 1 mV. The minimum resolution of the PSM with the OT 301 amplifier is therefore 0.5 mm.

The control mirror, beam splitters and folding mirrors are mounted on a Vibration Isolation Platform purchased from the Newport Corporation. An inertial actuator from CSA Engineering Inc., model SA-5, with a maximum 5 lb actuation force is used to induce vibrations in the platform. The entire system is mounted on a vibrationally isolated Newport Optical Bench.

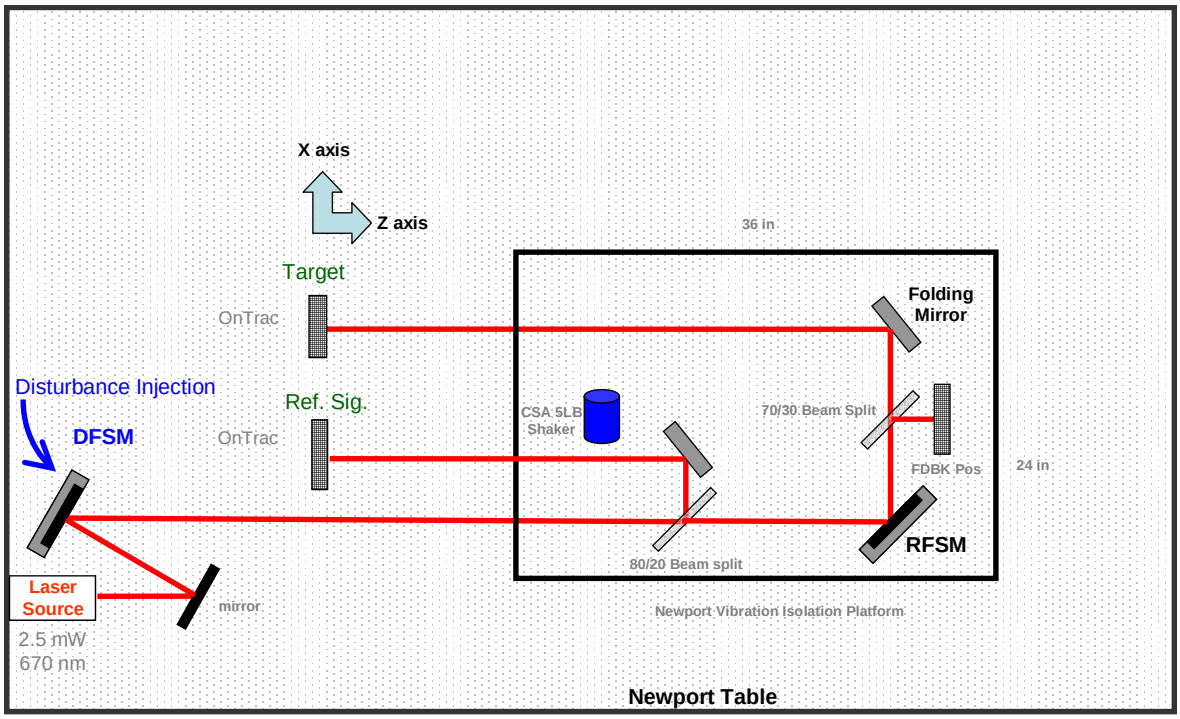

Figure 1: Laser Jitter Control Testbed

B. Mathematical model

In order to understand the setup in classical control terms, and thereby gain insight into the system, a mathematical model is constructed and control of the system using a Linear Quadratic Optimal Regulator (LQR) is first attempted. A simple second order transfer function of the Newport mirror about one axis is defined:

$$H_m(s) = \frac{\omega_n^2}{s^2 + 2\zeta\omega_n s + \omega_n^2} \quad (1)$$

where ωn=5000 rad/s (the experimentally determined value for the natural frequency of the Newport mirror) and ζ = 0.50. The damping ratio, ζ, was determined by comparing the model's frequency response to the actual frequency response of the mirror, and adjusting ζ accordingly. A delay was added to account for the time lag in the command circuitry to the mirror and the detection circuitry of the PSM/OT-301:

$$H_d(s) = \frac{1}{Ts + 1} \quad (2)$$

where T is roughly 0.00024 sec. The value for T was determined by comparing the step response of the experimental system to a simulated step response using the mathematical model, and adjusting T until the simulated and actual step responses matched. The resulting State-Space set of equations for one axis is given:

$$\begin{bmatrix} \dot{V}_p \\ \dot{\theta} \\ \ddot{\theta} \end{bmatrix} = \begin{bmatrix} -1/T & 2GpDm/T & 0 \\ 0 & 0 & 1 \\ 0 & -\omega_n^2 & -2\zeta\omega_n \end{bmatrix} \begin{bmatrix} V_p \\ \theta \\ \dot{\theta} \end{bmatrix} + \begin{bmatrix} 0 \\ 0 \\ \omega_n^2 Gm \end{bmatrix} V_m + \begin{bmatrix} -GpDb/T \\ 0 \\ 0 \end{bmatrix} \theta_d \quad (3)$$

In equation (3), V_p is the voltage at the PSM, Gp is the PSM gain, V/m, and D_m is the distance from the control mirror to the PSM, m. θ is the rotation about the control mirror's x axis, Gm is the control mirror gain, rad/V, and

V_m is the voltage input to the control mirror. D_b is the distance from the disturbance source to the detector and θ_d is the rotation about the laser beam's x or y axis at the disturbance source. θ_d is a pseudo-random variable, considered to be band-limited white noise plus any narrow-band disturbances.

III. Control Algorithms

In the sections below we summarize the control and signal processing algorithms we have implemented and tested for jitter rejection on the LJC testbed, including linear quadratic regulator (LQR) control, adaptive least mean squares (LMS) algorithm and gradient adaptive lattice algorithm. In this first attempt at controlling the FSM to compensate for broad-band and narrow-band disturbances, a single-input/single-output (SISO) system is employed with each axis of the disturbance and control mirror treated separately. As the research progresses, multiple-input/multiple-output (MIMO) systems will be utilized to investigate the ability to compensate for noise using MIMO control techniques. In developing these algorithms, care must be taken to solve for the discrete solution using the sample time of the computer control system, typically 0.0005 sec.

A. Linear Quadratic Regulator (LQR) Control

The LQR is first developed to investigate how classical control algorithms handle broadband disturbances. Using the State-Space system of equation (3), the optimal gains are determined using the algorithms available in MATLAB. The LQR requires full state feedback, which is not available for this system: the voltage from the detector and the position of the mirror can be measured, but not the velocity of the mirror. An observer, after the method of Friedland[5] was constructed to estimate the velocity of the mirror. The velocity may also be estimated by taking the derivative of the position, and after filtering, a usable signal was obtained using this method. Using either method resulted in satisfactory performance. A Kalman filter has been recently added which improved performance. The linear-quadratic optimal gains (K) were calculated to minimize

$$J = \int_0^\infty (x^T Q x + u^T R u) dt$$

the quadratic cost function with x being the state vector, and u the input. The matrices Q and R are used to weight the relative importance of each state and the input. The control law is $u = -Kx$. The state-space system defined in Sect. 2.2 is used to solve for the optimal gains for the LQR, with increased weighting on the voltage at the detector, Vp.

B. Adaptive Control

In adaptive control, we adjust the *tap gains* based on the response of the system to (1) the error, (2) a reference signal correlated with the disturbance, and (3) the control input. The algorithm may use (one of) various means, such as Least Squares or other stochastic methods, to find the optimum system. In particular, the algorithm relies on *predicting* its next input, which is simply the disturbance in the case of laser jitter control, to optimize the *tap gains*. The error - the difference between the predicted signal and the system output - is then used to recalculate the gains that minimize the error in return. For the LJC Testbed, the feed-back detector is used to provide the error signal, and the feed-forward detector provides the correlated disturbance input signal. This type of control algorithm not only calculates the necessary gains, but also identifies the system, removing the requirement to mathematically model the system. The type of adaptive control used in the experimental setup utilizes predictors. One type of *forward* predictor is the transversal or ladder filter, as shown in Figure 2. One may also conduct *backward prediction*, i.e. calculate what an input was in the past, given the n current and past inputs. Both the Least Mean Squares and Gradient Adaptive Lattice filters described in Sect. D and E below were modeled after *Haykin* in Ref. 6.

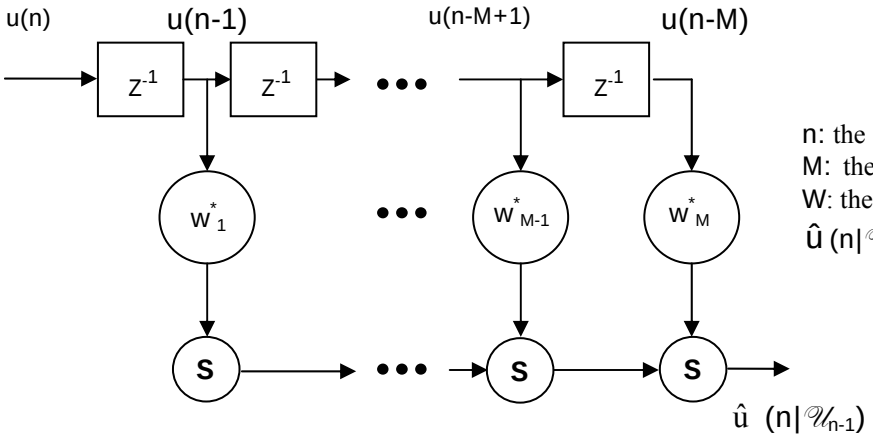

Figure 2. Transversal or ladder filter

C. Wiener filter

Using the Wiener-Hopf equations[6], we may determine the optimum tap gains w, for the filter shown in Figure 3, given the order of the filter, the inputs and the desired output. The optimum tap gain vector is then given by $w_f = R^{-1}p$, with R defined as the correlation matrix of delayed inputs and p the cross-correlation between delayed inputs and desired output. The output of this filter should give the best possible reduction in the amplitude of the disturbance.

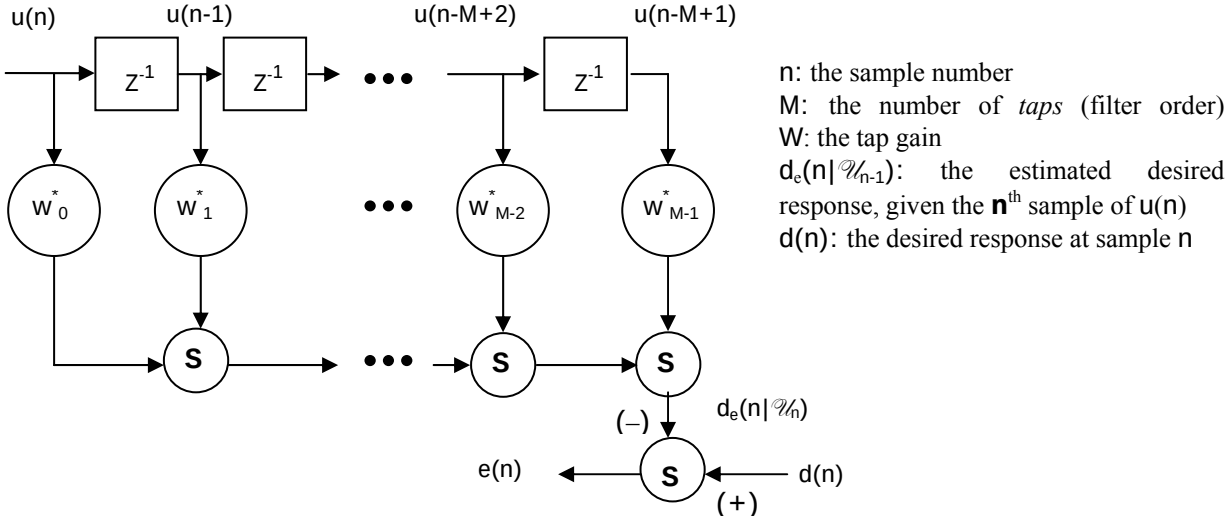

Figure 3. Compensation Scheme using the Ladder Filter

D. Adaptive least mean squares (LMS) algorithm

The LMS algorithm seeks to minimize or even cancel the effect of disturbance at the feedback PSM on the LJC testbed using the control mirror position. The tap gain vector, $\mathbf{W}_f$ (Figure 3) is computed using the error from the feedback PSM, vector of delayed disturbance inputs and an adaptation rate. The maximum adaptation rate, μ that can be used and maintain stability is $\mu \leq \lambda_{max}^{-1}$ where λ_{max} is the largest eigenvalue of the input correlation matrix[6,7]. The adaptation rate is determined experimentally to be the value that gave the overall best reduction in the amplitude of the disturbance. The algorithm used in this experiment is similar to that given in Ref. 7, 8 and 9, but no filtering on the disturbance correlated signal is performed due to the near unity characteristic of the system transfer function within the control bandwidth.

E. Gradient adaptive lattice (GAL) algorithm

The GAL algorithm uses both forward and backward prediction to develop the estimate of the desired cancellation signal, which again drives the control mirror to cancel the effect of disturbance input. The construction of the GAL filter is different than the linear transversal filter in that it uses reflection coefficients vice tap gains due to the nature of the *lattice-like* structure as shown in Figure 4. The forward prediction error for the i^{th} stage is given the symbol $f_i(n)$. The backward prediction error, b_i is given likewise. k is the reflection coefficient for the i^{th} stage and h_i provides the gains to construct the desired response, y_m. The h_i are calculated using the method of least squares, with the b_i as the regressor and the h_i as the parameters to be solved. The lattice filter results in a highly efficient structure in that it is modular. Each stage only requires the output of the previous stage, and an increase in the order of the filter only requires adding additional stages[6]. Ref. 10 and 11 discuss active noise cancellation techniques using algorithms that employ the lattice filter. The same concept was used in this study, but the algorithm from Ref. 6 was used due to its simpler implementation.

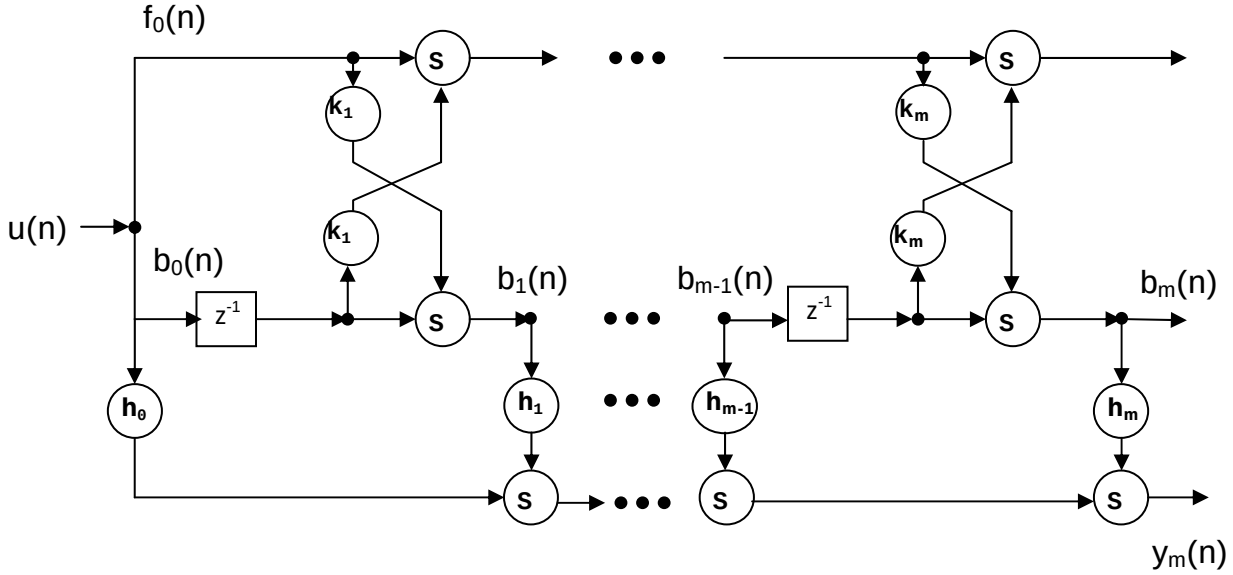

Figure 4. Lattice Filter

IV. Experimental Results for a Stable Platform

As the jitter spectrum of optical subsystems on spacecraft contain not only narrow band noise due to rotating devices such as reaction wheels but also broadband random noise, colored noise was used in our experiments to investigate the effectiveness of the control algorithms. The injected disturbance at the DFSM was 200 Hz band-limited white noise with two narrowband frequencies added in – one at 50 Hz and the second at 100 Hz. Other cases were tested in which non-harmonically related frequencies were used with very similar results. In this series of experiments, the platform was held stable. Both narrowband disturbance amplitudes were selected to be 25 mm at the feedback detector, placing it on the same order of magnitude as the broadband disturbance. The feedback detector was used as the target during this phase of the experiment. The narrow band disturbances about each axis were also displaced in phase from each other. For the experimental setup given here, 100 mm at the feedforward detector corresponds to about a 150 mrad rotation of the laser beam axis at the disturbance mirror. Both mirror axis were controlled independently at the same time, with each axis treated as a SISO system. Note that a rotation of the control mirror about the x-axis of the mirror results in a y-axis displacement at the feedback detector, and vice-versa. The standard deviation of the input disturbance at the feedforward detector and the output at the feedback detector were used as a measure of performance. The feed-back detector provides the error signal and the feed-forward detector provides the input. In each of the Adaptive LMS and GAL runs, the experiment was run for a minimum of 30 seconds, which was more than enough time to allow the gains to reach their steady-state values. The responses shown in the following figures are those for the experimentally determined optimum number of stages.

In the following four sections, the performance of the control algorithms is first presented. From Figure 5 to Figure 8, the left-hand figure is the time domain results, and the right-hand figure is their corresponding Power Spectral Density (PSD). The abscissa on the time domain graph indicates the position of the centroid of the laser

beam with respect to the center of the PSM, along each axis of the PSM. The input jitter is the beams position at the feedforward detector. The controlled beam is the position of the laser beam on the feedback detector. A one second period of data is shown. The PSD is only given for the x-axis, as each controller generated very similar frequency responses for each axis.

A. LQG control response

The LQG controller parameters were obtained using the State-Space model in Equation. 3 and initially using MATLAB to discretize the system and solve for the LQ-optimal gains. The sample time was 0.0005 seconds. The weighting matrix Q was constructed to give the state corresponding to the voltage at the feedback detector a weight of 1000 compared to 1 for the other two states. The input voltage to the control mirror was given a weight of 0.1 in the weighting matrix R. This resulted in a set of gains for each state, but the values were not optimum as evidenced by further experimentation. It is believed the difficulty in obtaining optimum gains using this method is due to the extremely stiff set of matrices used to model the system. Starting with these values and then using a trial an error approach, a set of gains were obtained that appear to be near the optimum in these experiments.

The LQG controller centered the beam on the feedback detector and reduced the amplitude of the input jitter by about 70 percent. The PSD shows the typical waterbed effect, with energy being added by the control system at frequencies above the control bandwidth, 200 Hz. It is apparent that the LQG controller does not discriminate between narrowband and broadband disturbance frequencies. As a result, the narrowband components at 50 Hz and 100 Hz are reduced merely by around 15 and 10 db, respectfully.

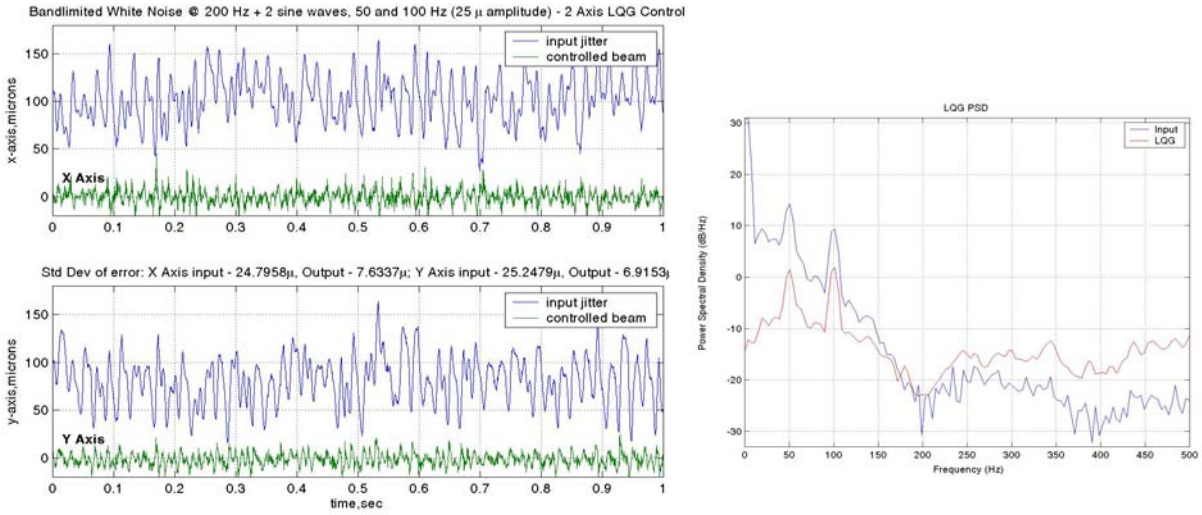

Figure 5. LQR Response

B. Wiener filter response

As a baseline for study of the adaptive filter, data taken from the experimentally induced jitter was filtered through the ideal Wiener filter offline, and the results presented in Figure 6. The power spectral density for the Weiner filter is also provided on each of the adaptive responses as a means of comparison. Only one axis is shown for the Weiner filter because the system behavior for both axes is almost identical for the LJC testbed. The Wiener filter indicates that the ideal adaptive filter should reduce the amplitude of the input jitter by 85 percent with about 25 db and 20 db decreases in the PSD of the two narrowband components, respectfully.

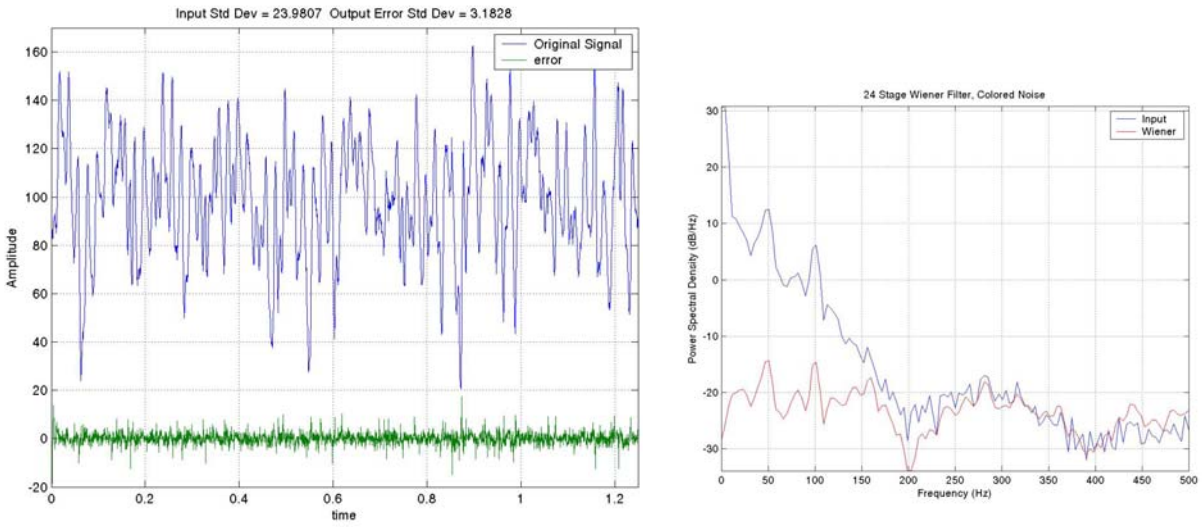

Figure 6. Wiener Filter Response

C. Adaptive LMS control response

The LMS controller was developed using the LMS adaptive filter from the Digital Signal Processing Toolbox of MATLAB. An adaptation rate of 0.1 was determined to be optimum for both axes by experimentation. A value of 1.0 for the leakage factor provided the best results. The LMS controller performed well for the colored noise disturbance, approaching the Weiner filter values. LMS control resulted in a greater than 80 percent decrease in the input jitter.

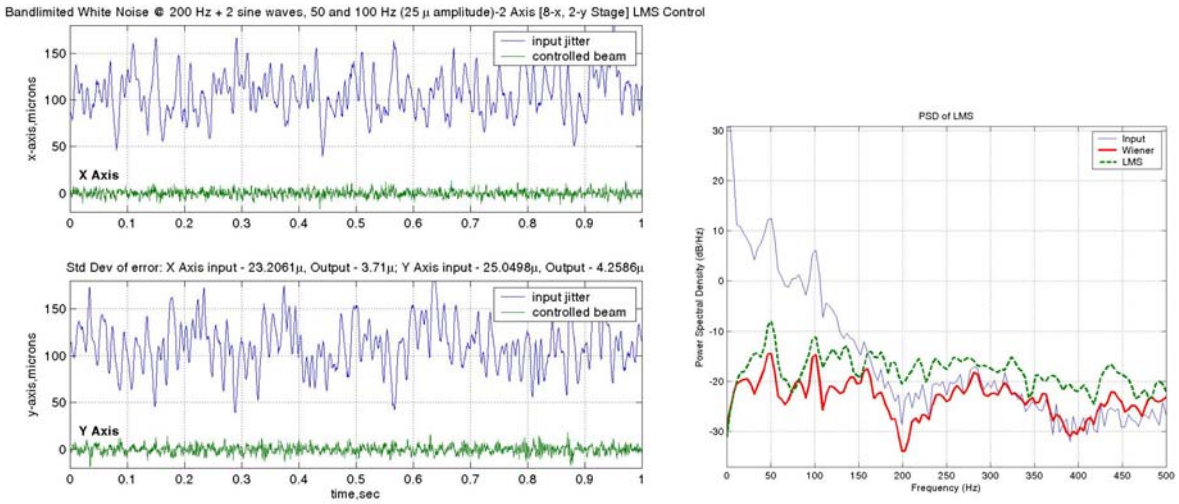

Figure 7. LMS response

D. GAL control response

The GAL algorithm was developed from that given in Table 12.1 of Ref. 6. The small, positive constants required by this algorithm, δ and a were set to 0.01. The "forgetting factor", β, was set to 0.5, and μ, the adaptation rate, was 0.01. The algorithm was coded in C language into an "S-function" for use in the Real Time Workshop required for xPC Target[3].

The GAL algorithm achieved about a 75 percent reduction in the input jitter, not too much better than the LQR controller. This may be due to approximate nature of the GAL algorithm as described in Ref. 6. A more stringent order-recursive lattice filter may provide better results and is the subject of further studies.

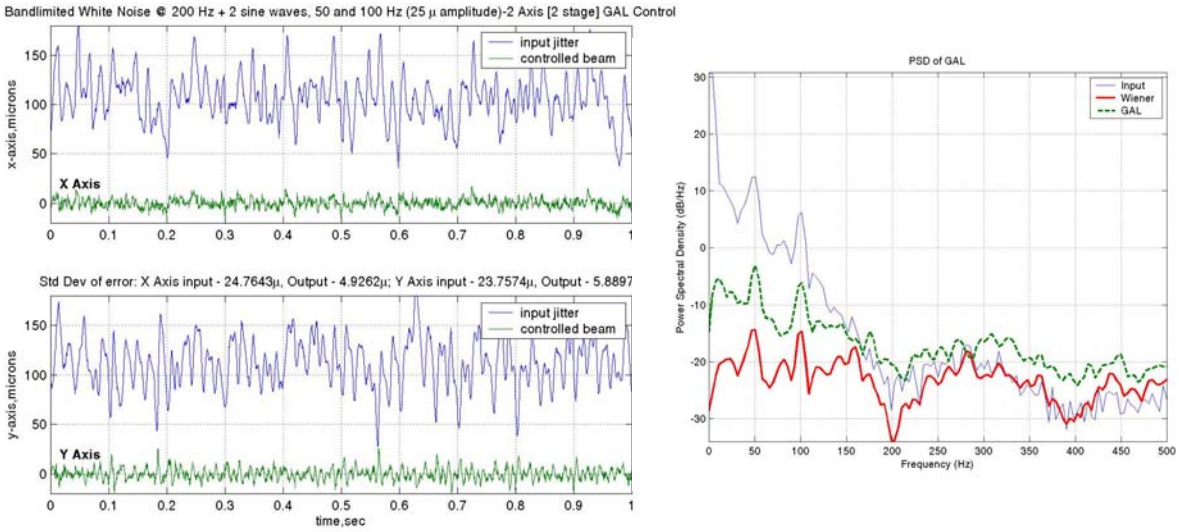

Figure 8. GAL response

E. GAL/LQG/LMS comparison

The results obtained in all previous sections are put together here for comparison. Figure 9 shows that both adaptive algorithms, LMS and GAL, achieve superior performance than that of the LQG method in suppressing the injected colored noise, with the LMS algorithm's performance very close to that of the ideal Wiener filter. The standard deviation of both the effect of the input jitter and the response of all three controllers on each axis are summarized in Table 1.

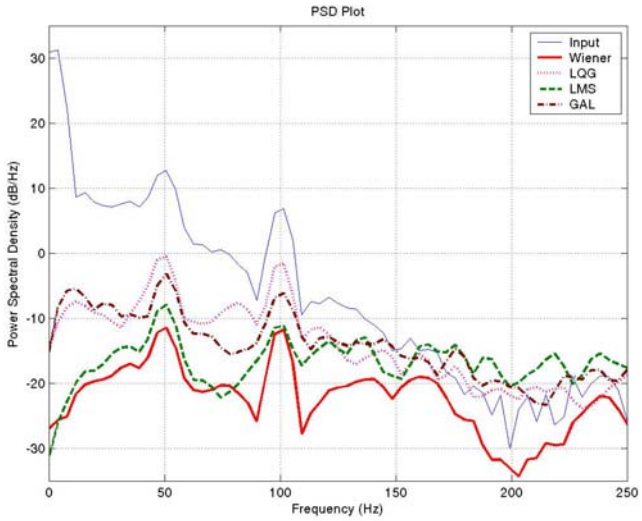

Figure 9. PSD of LQG, LMS, and GAL compared to the Wiener Filter

Table 1. Comparison of Controllers

Controller	LQG		LMS		GAL	
Control Mirror Axis	X-axis	Y-axis	X-axis	Y-axis	X-axis	Y-axis
Input Jitter, Std. Dev, mm	24.8	25.2	23.2	25.0	24.8	23.8
Controlled Beam, Std Dev., mm	7.6	6.9	3.7	4.3	4.9	5.9
No. of stages/order	n/a	n/a	8	2	2	2
% reduction in jitter	69	73	84	83	80	75
db reduction in PSD of 50 Hz	-12	-12	-20	-20	-16	-16

F. Optimal stage number for adaptive algorithms

A series of experiments were conducted to determine the optimum filter order for the LMS filter and the optimum number of stages for the GAL filter. The percent reduction achieved in correcting the input jitter is plotted versus the number of stages (GAL) or order (LMS) of the adaptive filter. As is apparent from Figure 10, the LMS filter outperformed the GAL filter, regardless of the number of stages. The average execution time for each step was also documented to observe how efficient each algorithm was. In our current implementation, as can be seen from the graph, the execution time of the GAL algorithm rapidly approached the discrete sample time of 500 micro-seconds, and in fact the controller was unable to execute a 64 stage filter due to the execution time exceeding the sample time. The LMS algorithm stayed essentially constant as the order was increased. It is also interesting to note that as the execution time for the GAL algorithm increased, the ability to control the jitter decreased. This contradicts the general notion that the GAL algorithm, using lattice filters, yields a better computational efficiency than LMS algorithm, and therefore requires further study.

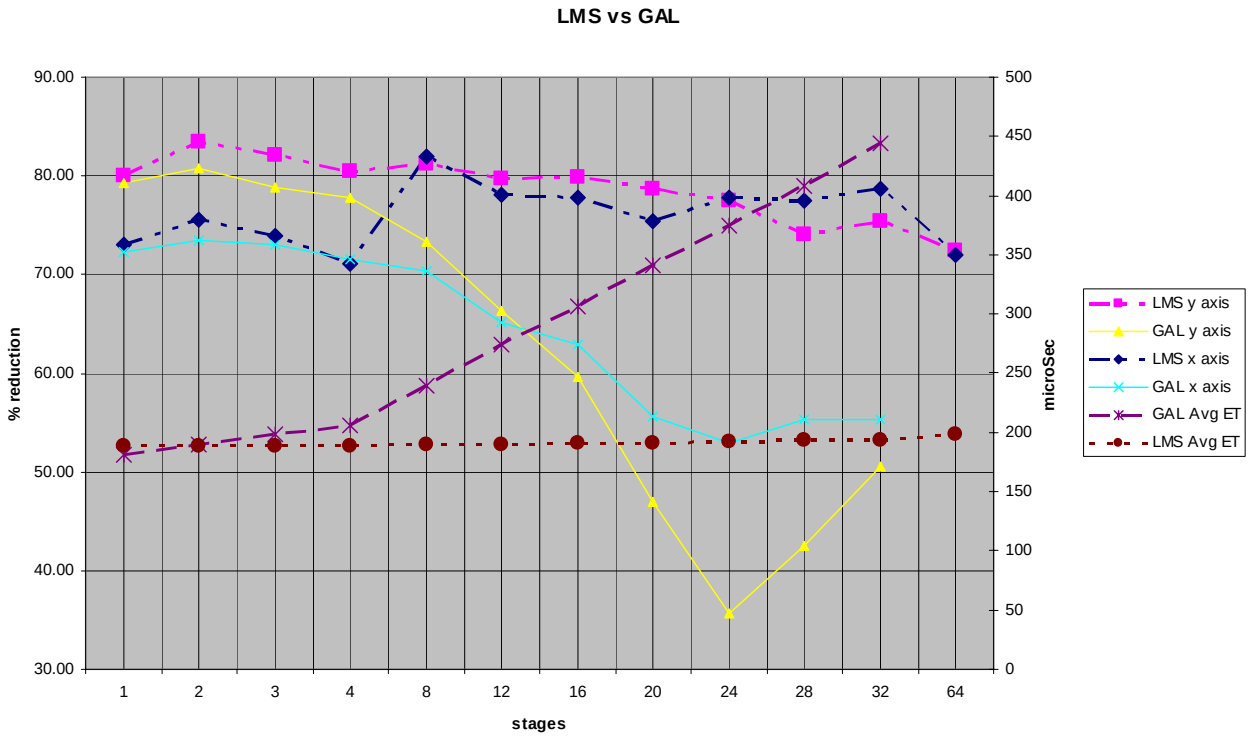

Figure 10. Percent reduction (in individual axis) and execution time (of each algorithm) vs. No. of Stages

V. Experimental Results with a Vibrating Platform

In the next set of experiments, the platform containing the control system is shaken to determine the effects of onboard disturbances. The feedback was shifted to the target PSD, positioned off the platform, approximately 1.2 m from the control mirror. The addition of a vibrating platform resulted in a significantly more complex control environment. The shaker was oriented to vibrate the platform in the x-z plane, in the x direction at 37.5 Hz (see Fig. 1). However, the mounting of the shaker allowed vibrations in the x-y plane as well, as can been seen from Figure 11. In order to provide the largest amplitude vibrations for the platform, 37.5 Hz was selected based on the response characteristics of the CSA shaker. The structure attenuates the vibration as can also be seen in Figure 11. In each of the control runs, the platform was allowed to shake for 1 second with no control inputs, and the data from the target PSD was recorded to ensure an accurate comparison of uncontrolled vs. controlled results. Figure 11 gives a sample of the uncontrolled vibrations at both the reference PSD and the target PSD.

Vibration of the platform also results in a problem in determining the reference signal for the LMS controller. For the small vibrations we were using, our accelerometers were extremely noisy and unusable from the standpoint of control in the range of motion we desired. For the initial investigation, we decided to assume an inertial reference signal would be available for the controller. In order to simulate this, the reference PSD was placed off the platform, and the laser beam was split and reflected to this PSD. In this manner, an accurate inertial reference signal was obtained.

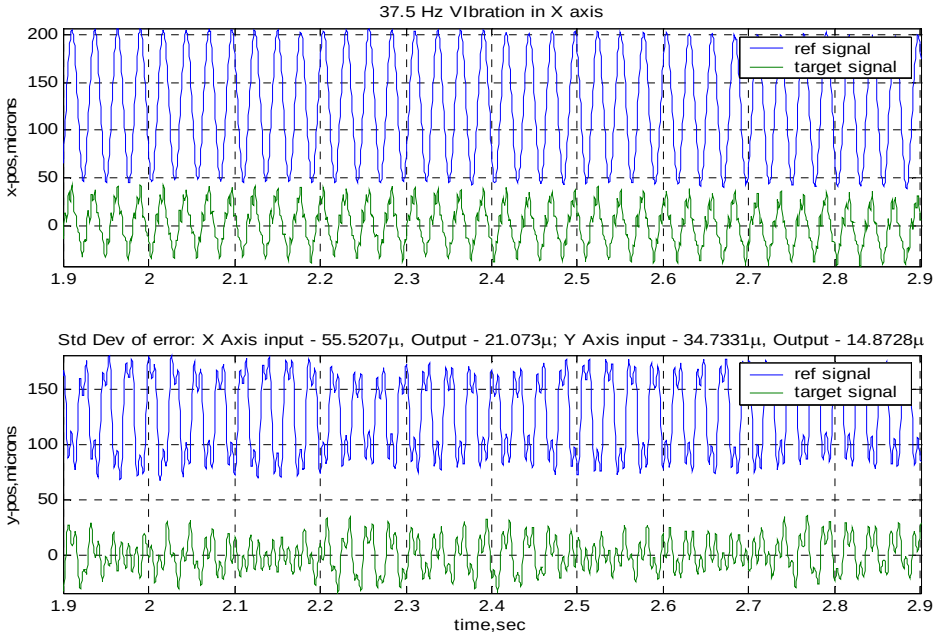

Figure 11. 37.5 Hz vibration of platform with no control

The addition of 200 Hz band-limited white noise from the DFSM further complicated the spectrum as can be seen in Figure 12.

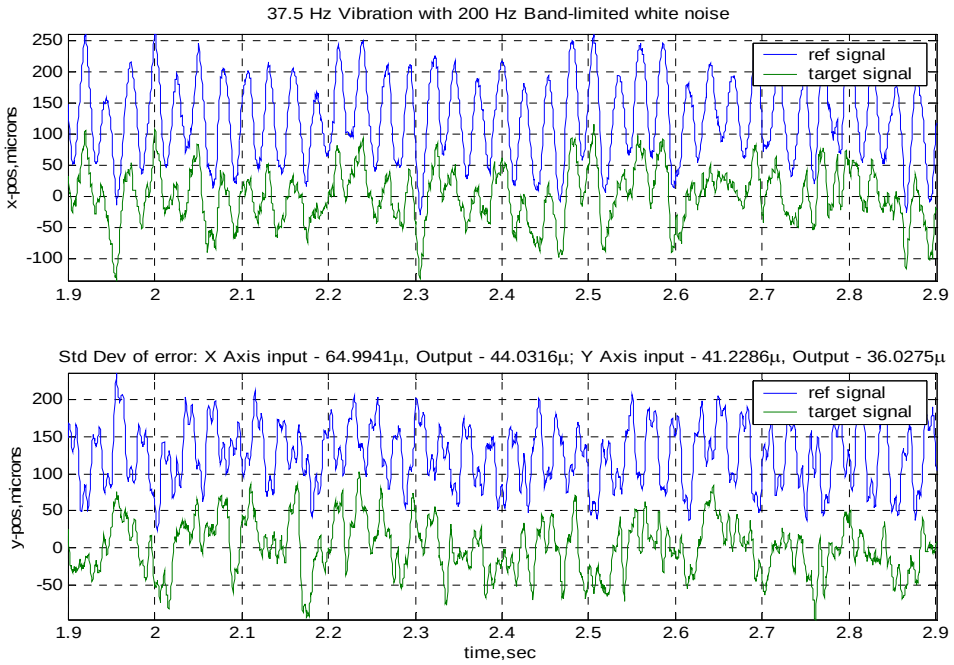

Figure 12. Disturbance signal generated by 37.5 Hz vibration of platform and 200 Hz noise from DFSM

A. LQG Control of vibrating platform disturbance

The LQG controller was retuned for the vibrating platform and the results are shown in Fig. 13 for the case with no noise from the DFSM. Fig. 14 shows the case with 200 Hz random noise from the DFSM. Bias errors were not corrected.

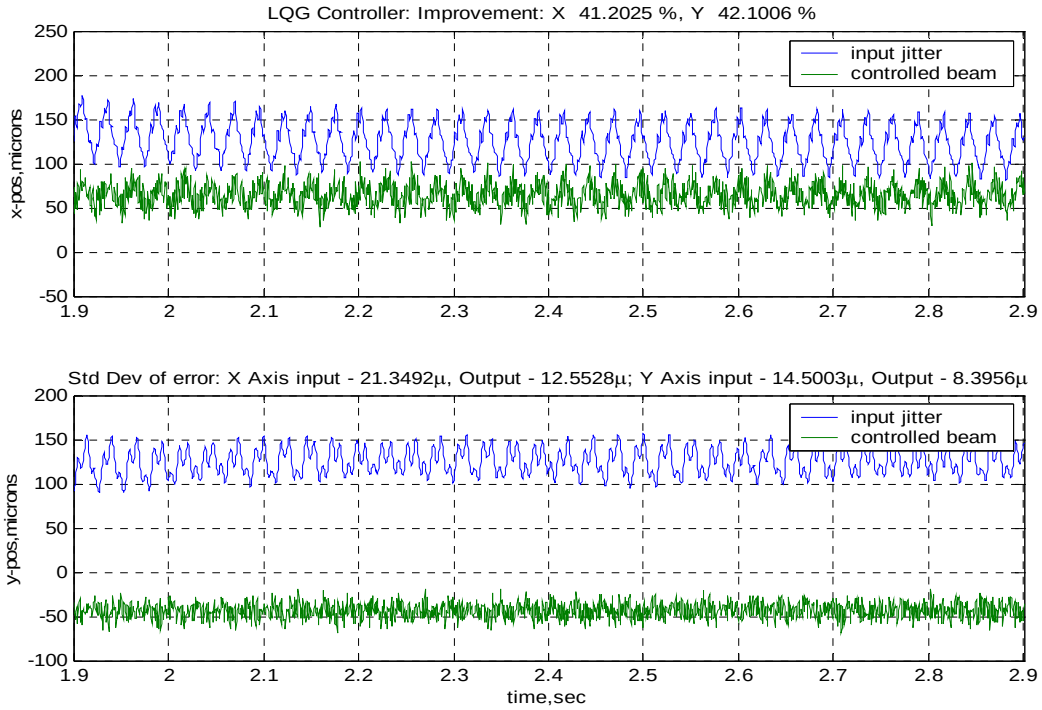

Figure 13. LQG control of beam with 37.5 Hz vibrating platform

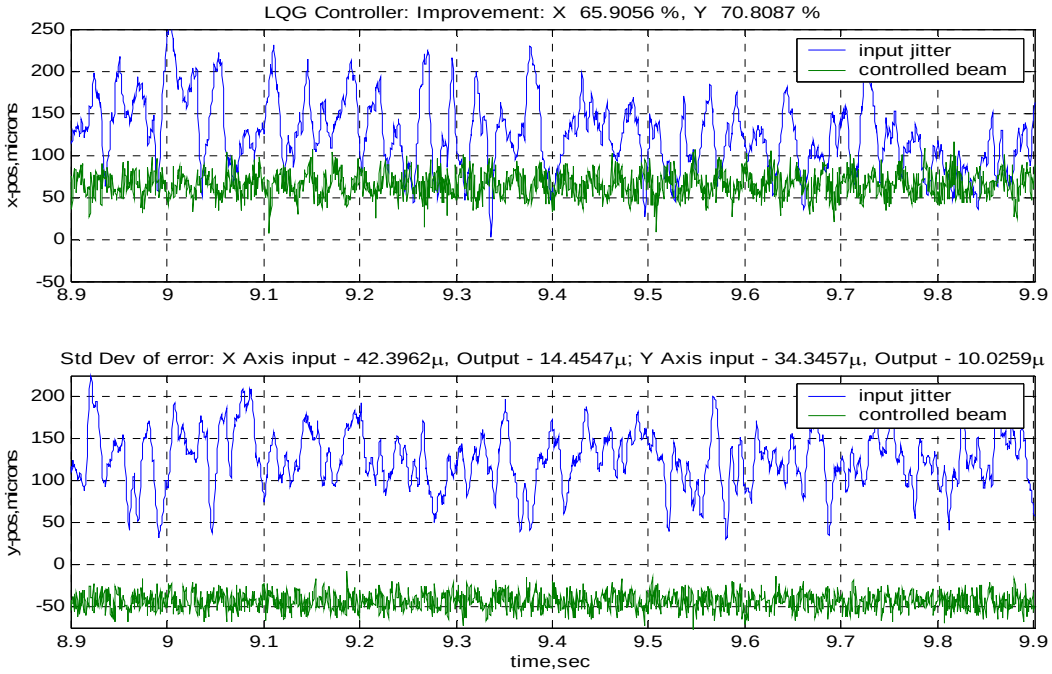

Figure 14. LQG control of beam with 37.5 Hz vibration and 200 Hz noise from DFSM

B. LMS Control of vibrating platform disturbance

A Filtered-X version of the LMS controller was built for this next phase of the experiment. Filtering the reference signal with an estimate of the mirror transfer function was evaluated to determine the effect of this method. A block diagram of the controller is given in Fig. 15 below. A second order model, similar to the one given in equation (1) above was used to model the mirror's transfer function. In this series of experiments, the order of the LMS filter was held constant at 12.

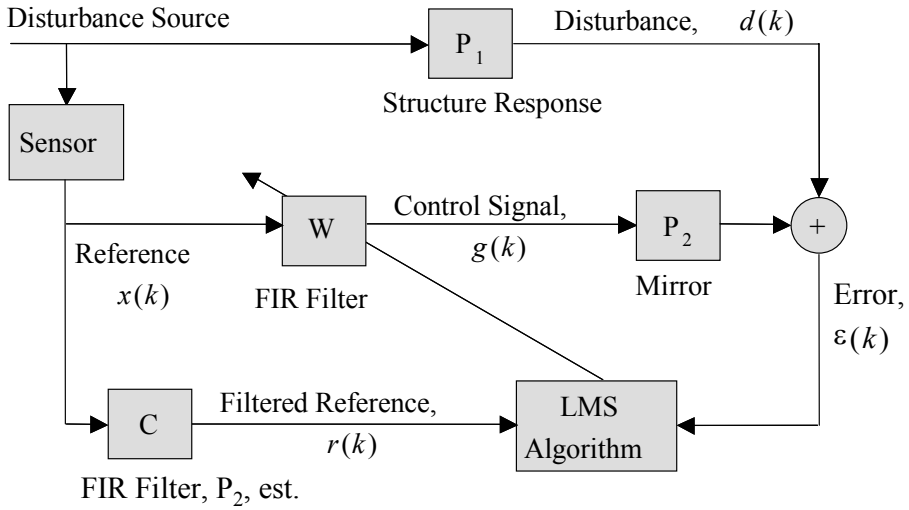

Figure 15. Filtered-X LMS controller

The Filtered-X version resulted, in general, in a small increase (1-4%) in the ability of the controller to reduce the jitter at the target PSD. Further study of this controller is required to quantify the results of the filtered vs. non-filtered version. The results depicted in this phase of the experiment are all of the Filtered-X version of the controller.

Fig. 16 shows the LMS control of the system with no input noise from the DFSM.

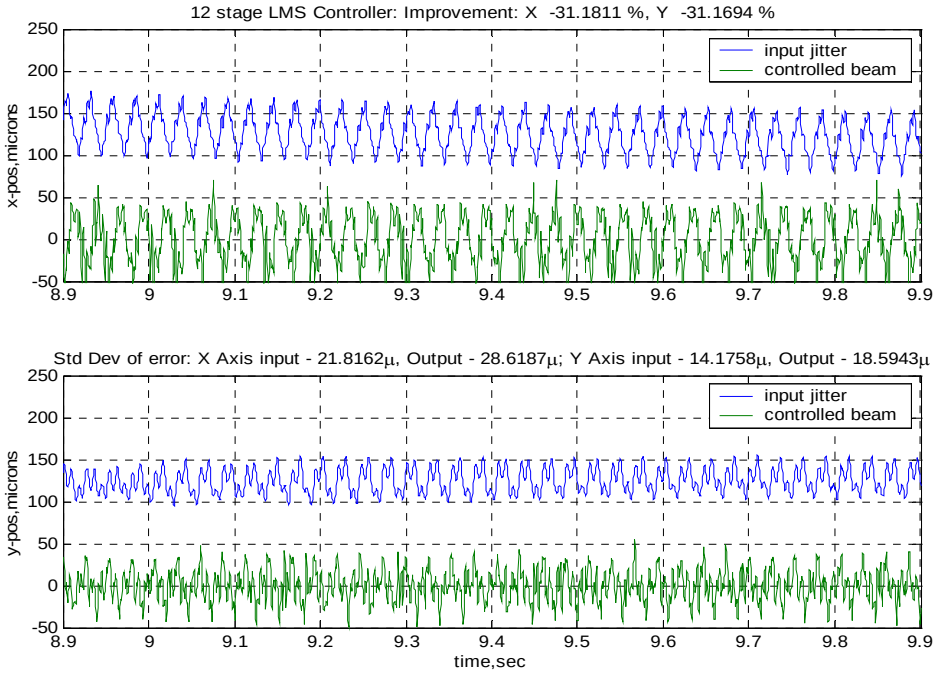

Figure 16. Filtered-X LMS control of beam with 37.5 Hz vibrating platform

LMS control results in an increase in the standard deviation of the beam at the target PSD. Further research is required into determining why the effect of vibrating the platform causes the LMS controller to increase the amplitude of the input jitter. However, it is noted that the beam is controlled around the center of the target PSD. Fig. 17 shows the effect of Filtered-X LMS control with input noise from the DFSM in addition to the vibration of the platform.

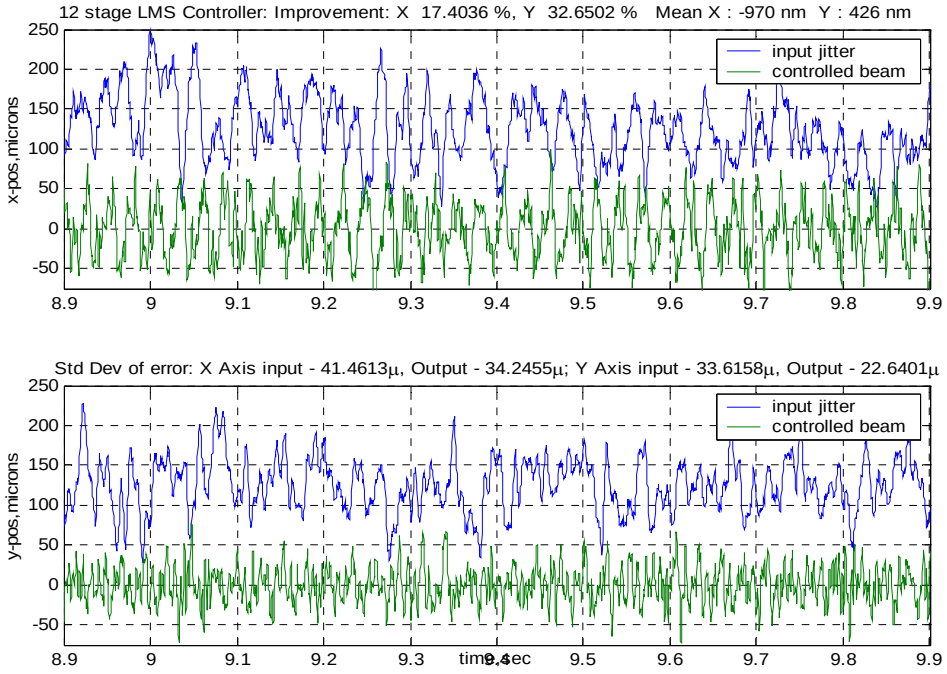

Figure 17. Filtered-X LMS control of beam with 37.5 Hz vibration and 200 Hz noise from DFSM

The LMS controller shows a slight reduction in the jitter at the target, but not as much as that seen with no vibration on the platform. The LQG controller shows better response than the LMS controller in this case, however, the LMS controller has centered the beam to less than 1 mm.

C. LQG plus LMS Control of vibrating platform disturbance

Experiments were conducted with the LQG controller in parallel with the Filtered-X LMS controller. This control combination takes advantage of the LQG controller's superior performance in reducing the disturbance amplitude, (in the case of a vibrating platform), with the LMS ability to remove the bias in the signal. The results are shown in Fig. 18 and 19. Both figures show the ability of the controller to center the beam very accurately on the target sensor, within the resolution capability of the PSD (500nm). The addition of LMS control to the LQG controller has very little effect on the ability of the LQG controller to compensate for the vibration and random noise.

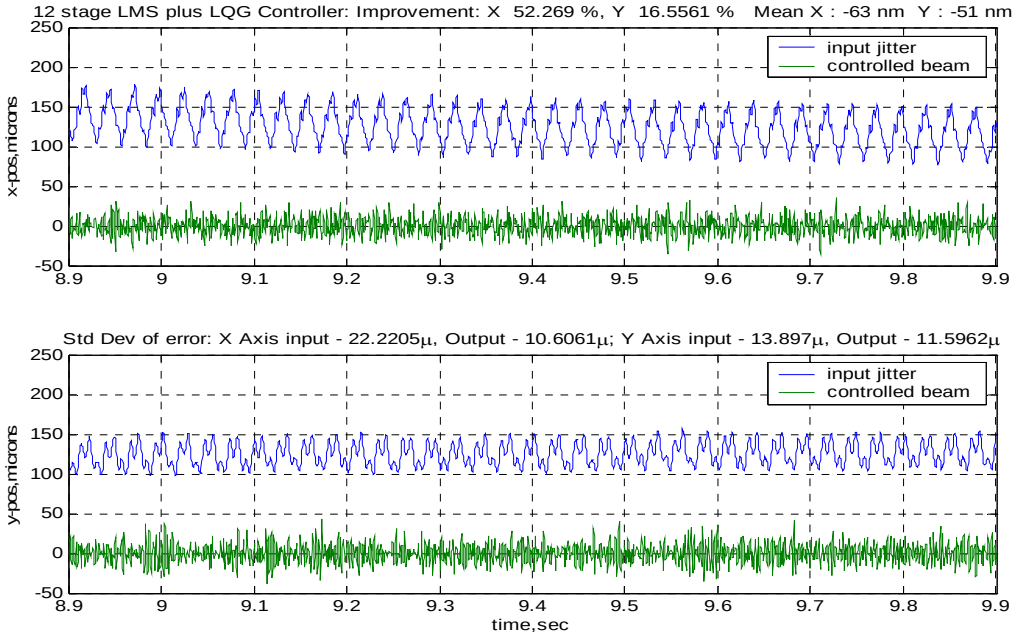

Figure 18. LMS plus LQG control of beam with 37.5 Hz vibrating platform

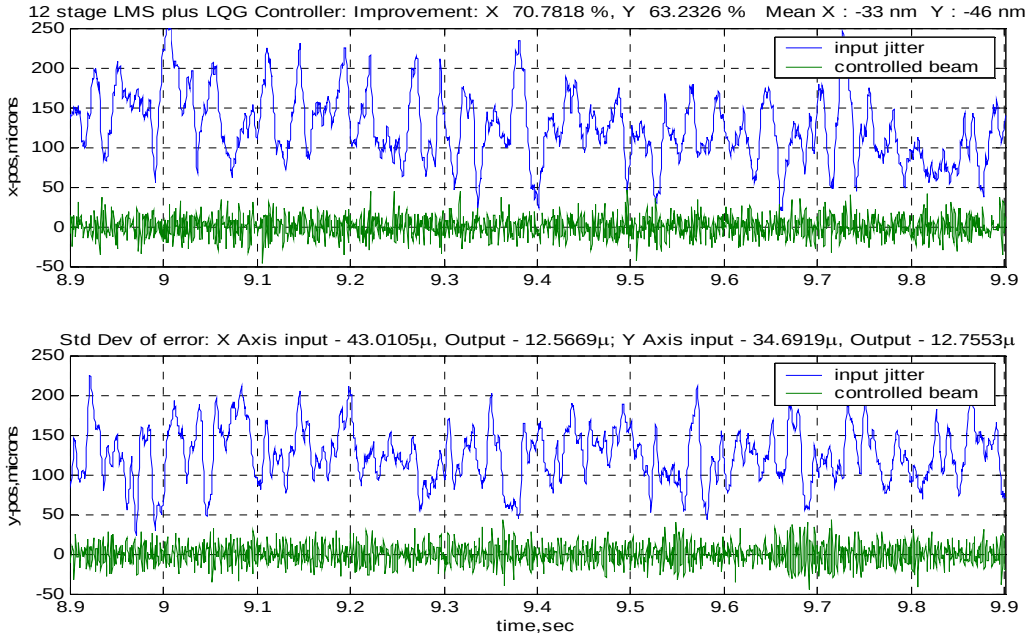

Figure 19. LMS plus LQG control of beam with 37.5 Hz vibration and 200 Hz noise from DFSM

D. Comparison of Controllers

Table 2 compares each of the individual controllers, as well as the combined systems. Experiments with the GAL controller from phase 1 were conducted with similar results to the LMS controller, however the data was very preliminary and further study is needed to refine and quantify these results.

Table 2. Comparison of Controllers, Vibrating Platform with Random Noise from DFSM

Controller	LQG		LMS		LMS+LQG	
Control Mirror Axis	X-axis	Y-axis	X-axis	X-axis	X-axis	Y-axis
Input Jitter, Std. Dev, mm	42.4	34.3	41.4	33.6	43	34.7
Controlled Beam, Std Dev., mm	14.5	10.0	34.2	22.6	12.6	12.8
No. of stages/order	n/a	n/a	12	12	12	12
% reduction in jitter	65.9	70.8	17.4	32.7	70.8	63.2

VI. Conclusions

A laser jitter control testbed has been constructed and three control algorithms have been tested on their effectiveness in suppressing the effect of injected colored noise. The initial experiments on a stable platform indicate that both adaptive LMS and GAL algorithms result in better jitter reduction than does the classical LQG control method, using a second order system model in determining the LQ-optimal gains. A better LQG controller would most certainly be obtained by using a more exact higher order model. However, the adaptive schemes, which do not rely on mathematical models, should still perform at least as well, if not better than the LQG. In our current implementation, GAL does not show the predicted advantage over the LMS: GAL's performance decreases and execution time increases rapidly with the stage number while those of the LMS stay about the same.

A much more difficult problem results for the adaptive schemes when the supporting platform for the control mirror is vibrated. The adaptive systems, as configured, tend to add energy to the beam, resulting in additional jitter. The LQG system admits better control in this environment. It is postulated that some filtering of the reference signal is required to compensate for the phase shift or distortion that occurs between the reference signal and the output at the target. Testing with simple models indicate that a phase shift of the reference signal can enhance the ability of an LMS controller in this environment, but more work is needed to quantify the results and apply them to the

experimental setup. LMS control can be used with LQG control to effectively diminish the effects of a vibrating structure coupled with a random noise input independent of the induced vibrations.

Acknowledgments

The authors wish to acknowledge the help of Prof. Roberto Cristi for his insights into adaptive filter theory.

References

[1]Baker Adaptive Optics Homepage: http://www.flash.net/~jtbaker/

[2]Newport Corp. Fast Steering Mirror webpage: http://www.newport.com/semi/Products/Optics/product.asp?id=3881

[3]The Mathworks Inc., xPC Target webpage: http://www.mathworks.com/products/xpctarget/

[4]On-Trak Photonics Inc., Position Sensing Modules webpage: http://www.on-trak.com/psm.html

[5]B. Friedland, Control System Design: An Introduction to State-Space Methods, McGraw-Hill, New York, 1986

[6]S. Haykin, Adaptive Filter Theory, Prentice-Hall, New Jersey, 2002

[7]Widrow, B. and Stearns, S.D., Adaptive Signal Processing, Prentice-Hall, New Jersey, 1985

[8]Edwards, S.G., "Active Narrowband Disturbance Rejection on an Ultra Quiet Platform", Dissertation, Naval Post Graduate School, Monterey, CA, 1999.

[9]H. J. Chen, R. W. Longman, B. N. Agrawal, M. Q. Phan, S. G. Edwards, "Rejection of Multiple Unrelated Periodic Disturbances Using MELMS with Disturbance Identification," Advances in the Astronautical Sciences, Vol. 108 (Part I), 2001, Proceedings of the 11th AAS/AIAA Space Flight Mechanics Meeting, Feb 11-15 2001, Santa Barbara, CA, p 587-606.

[10]Jiang S.-B. and Gibson, J.S., "An Unwindowed Multichannel Lattice Filter with Orthogonal Channels", IEEE Transactions on Signal Processing, Vol. 43, No. 12, pp 2831-2842, 1995

[11]Chen, S.-J. and Gibson, J.S., "Feedforward Adaptive Noise Control with Multivariable Gradient Lattice Filters", IEEE Transactions on Signal Processing, Vol. 49, No. 3, pp 511-519, 2001